Desalination and Water Treatment
www.deswater.com

doi: 10.1080/19443994.2015.1060166

57 (2016) 13404–13414
June

Taylor & Francis
Taylor & Francis Group

Effect on membrane fouling and intrinsic characteristics of UF subjected to potassium permanganate pre-oxidation

Zhe Wang[a,b], Tao Lin[a,b,*], Wei Chen[a,b,*]

[a]*Ministry of Education Key Laboratory of Integrated Regulation and Resource, Development on Shallow Lakes, Hohai University, Nanjing 210098, P.R. China, Tel. +86 13815437675; email: 876723019@qq.com (Z. Wang), Tel. +86 13951690290; email: hit_lintao@163.com (T. Lin), Tel. +86 13913899869; email: cw5826@hhu.edu.cn (W. Chen)*
[b]*College of Environment, Hohai University, Nanjing 210098, P.R. China*

Received 11 November 2014; Accepted 3 June 2015

ABSTRACT

The Extended Derjaguin–Landau–Verwey–Overbeek approach was used to investigate the mechanism of membrane fouling control with potassium permanganate ($KMnO_4$) pre-oxidation in an ultrafiltration (UF) system. The polymeric membrane, made of polyvinylidene fluoride (PVDF), was selected as membrane material in the investigation. Results demonstrated that $KMnO_4$ pre-oxidation increased the hydrophilicities of both membrane material and organic colloid and that the absolute value of calculated total interaction energy decreased by 33.5 and 33.6%, respectively, indicating the amelioration of membrane fouling. The results of transmembrane pressure and membrane resistance confirmed the mitigation of membrane fouling. It was found that the average pore size of the membrane material was decreased when UF system was subjected to $KMnO_4$. The characteristics of influent organic colloids were changed due to $KMnO_4$ pre-oxidation.

Keywords: Ultrafiltration; Potassium permanganate; Pre-oxidation; XDLVO approach; Contact angle; Membrane fouling

1. Introduction

Membrane technology has been widely used in the environmental protection [1], pharmaceutical industries [2], and water treatment [3,4]. Ultrafiltration (UF) technique has attracted considerable attention due to its capacity to produce pathogen-free filtrate in drinking water supplies [5–8], more effective in reducing pathogenic risk than the conventional sand filtration method [9,10]. Nevertheless, membrane fouling is a serious impediment to using UF as a substitute for conventional drinking water treatment processes. Natural organic matters (NOMs) have been regarded as major contributors to membrane fouling [11,12]. The inevitable NOM in the feed water to a UF system is the main cause of membrane fouling. The development of effective methods to remove or transform NOM is essential for the broader application of membrane technology in water treatment systems [13]. The pretreatment of feed water is often used for the removal of NOM to alleviate membrane fouling [14]. Pre-oxidation, an effective pretreatment method, has been widely used to remove or change the properties of NOM [15–18]. Previous studies have demonstrated that the pre-oxidation of feed water significantly mitigates membrane fouling, which is primarily attributed

*Corresponding authors.

to changes of NOM molecular characteristics [19,20]. H_2O_2/UV pre-oxidation of raw water significantly reduces membrane fouling by transforming hydrophobic NOM into hydrophilic fractions [21]. Potassium permanganate ($KMnO_4$) has been widely used in pre-oxidation process to remove the precursors of disinfection by-products in water. Pre-oxidation of UF feed water using $KMnO_4$ has alleviated membrane fouling [10,20]; in addition, the control mechanisms of membrane fouling have been investigated when the feed water is pre-oxidized with $KMnO_4$. However, how $KMnO_4$ pre-oxidation affects the characteristics of membrane material, such an important index as the contact angle, is yet not clear.

In aqueous solutions, NOM usually bonds together to form colloidal aggregates of tens or hundreds of nanometers in size. The attachment of a colloidal particle to a surface can be described using the Extended Derjaguin–Landau–Verwey–Overbeek (XDLVO) theory [21,22]. The XDLVO approach has been used to predict the interaction energy caused by organic colloids attached to the membrane surface [23]. Positive interaction force represents a repulsive action to reject membrane fouling, while a negative one causes an attraction to aggravate fouling [24]. Previous studies have shown that the interaction energy is strongly correlated with membrane resistance, indicating that the XDLVO approach can effectively predict membrane fouling [25]. However, there are few literatures on the investigations, using XDLVO approach, on membrane fouling and especial membrane material characteristics when UF system is subjected to $KMnO_4$ pre-oxidation.

In this study, the XDLVO theory was applied to predict membrane fouling to explore the effect mechanisms of $KMnO_4$ pre-oxidation of feed water, including its influence on the characteristics of aqueous colloids and the contact angle of membrane material.

2. Material and methods

2.1. XDLVO approach for interaction energy calculation

The XDLVO theory takes the following three interactions into consideration (as membrane fouling contributors): van der Waals (LW) interaction, electrostatic (EL) interaction, and short-ranged acidic–basic (AB) interaction. It describes the total interaction energy, or adhesion energy, between a colloid and a membrane surface as the sum of LW, AB, and EL interaction.

$$U_{\mathrm{mlc}}^{\mathrm{XDLVO}} = U_{\mathrm{mlc}}^{\mathrm{LW}} + U_{\mathrm{mlc}}^{\mathrm{EL}} + U_{\mathrm{mlc}}^{\mathrm{AB}} \tag{1}$$

where U^{XDLVO} is the total interaction energy between a membrane surface and a colloid immersed in water, U^{LW} is the LW interaction term, U^{EL} is the EL interaction term, and U^{AB} is the AB interaction term. The subscripts ""m", "l" and "c" correspond to the membrane, the bulk feed solution, and the colloid, respectively. The interaction energy is calculated according to the surface energy γ^{LW}, γ^{+}, γ^{-}, and γ^{AB} corresponding to Lifshitz–van der Waals, electron acceptor, electron donor, and acid–base, respectively [26].

The LW interaction energy between a membrane surface and a colloid in an aqueous environment can be expressed as follows [22]:

$$U_{\mathrm{mlc}}^{\mathrm{LW}}(y) = 2\pi\Delta G_{y_0}^{\mathrm{LW}} \frac{y_0^2 a_{\mathrm{c}}}{y} \tag{2}$$

where y_0 is the minimum equilibrium cutoff distance ($y_0 = 0.158 \pm 0.009$ nm); y is the separation distance between the flat plate (membrane) and the sphere (colloid), expressed in nm; a_{c} is the radius of the spherical colloid, expressed in nm; and $\Delta G_{y_0}^{\mathrm{LW}}$ is the LW adhesion energy per unit, expressed in $\mathrm{mJ/m^2}$.

The AB interaction energy between a membrane surface and a colloid can be expressed as follows [22]:

$$U_{\mathrm{mlc}}^{\mathrm{AB}} = 2\pi a_{\mathrm{c}} \lambda \Delta G_{y_0}^{\mathrm{AB}} \exp\left[\frac{y_0 - y}{\lambda}\right] \tag{3}$$

where λ is the characteristic decay length of AB interaction in water ($\lambda = 0.6$ nm) and $\Delta G_{y_0}^{\mathrm{AB}}$ is the AB adhesion energy per unit, expressed in $\mathrm{mJ/m^2}$.

The EL interaction energy between a membrane surface and a colloid in an aqueous environment is expressed as follows [22]:

$$U_{\mathrm{mlc}}^{\mathrm{EL}}(y) = \pi\varepsilon_0\varepsilon_{\mathrm{r}} a_{\mathrm{c}} \left(2\zeta_{\mathrm{c}}\zeta_{\mathrm{m}} \ln\left(\frac{1+e^{-\kappa y}}{1-e^{-\kappa y}}\right) + \left(\zeta_{\mathrm{c}}^2 + \zeta_{\mathrm{m}}^2\right) \ln\left(1 - e^{-2\kappa y}\right) \right) \tag{4}$$

where $_{0\mathrm{r}}$ is the dielectric permittivity of the suspending fluid ($_{0\mathrm{r}} = 6.95 \times 10^{-10}\ \mathrm{C^2\,J^{-1}\,m^{-1}}$); κ is the inverse Debye screening length ($\kappa = 0.104\ \mathrm{nm^{-1}}$); and ζ_{c} and ζ_{m}, expressed in mV, are the surface potentials of a membrane and a colloid, respectively.

When the separation between two surfaces is close to the minimum equilibrium cutoff distance, the LW/AB adhesion energy per unit can be expressed as below [25]:

$$\Delta G_{y_0}^{\mathrm{LW}} = 2\left(\sqrt{\gamma_{\mathrm{l}}^{\mathrm{LW}}} - \sqrt{\gamma_{\mathrm{m}}^{\mathrm{LW}}}\right)\left(\sqrt{\gamma_{\mathrm{c}}^{\mathrm{LW}}} - \sqrt{\gamma_{\mathrm{l}}^{\mathrm{LW}}}\right) \tag{5}$$

$$\Delta G_{y_0}^{AB} = 2\sqrt{\gamma_l^+}\left(\sqrt{\gamma_m^-} + \sqrt{\gamma_c^-} - \sqrt{\gamma_l^-}\right) + 2\sqrt{\gamma_l^-}\left(\sqrt{\gamma_m^+} + \sqrt{\gamma_c^+} - \sqrt{\gamma_l^+}\right) - 2\left(\sqrt{\gamma_m^+\gamma_c^-} + \sqrt{\gamma_m^-\gamma_c^+}\right) \quad (6)$$

where γ^{LW}, γ^+, and $\gamma^-$are the surface tension parameters, expressed in mJ/m^2;

Surface energy can be calculated using the contact angle parameter and the acid–base approach. The contact angle of a liquid on a solid surface can be expressed as follows [17]:

$$\gamma^{TOT} = \gamma^{AB} + \gamma^{LW} \quad (7)$$

$$\gamma^{AB} = 2\sqrt{\gamma^+\gamma^-} \quad (8)$$

$$\left(\gamma_L^{LW} + 2\sqrt{\gamma_L^+\gamma_L^-}\right)(1+\cos\ \theta) = 2\left(\sqrt{\gamma_S^{LW}\gamma_L^{LW}} + \sqrt{\gamma_S^+\gamma_L^-} + \sqrt{\gamma_S^-\gamma_L^+}\right) \quad (9)$$

where θ is the contact angle. The surface tension parameters (γ_S^{LW}, γ_S^+, and γ_S^-) of a solid can be obtained by determining the contact angles between the solid and three probe liquids with well-known surface tension properties (γ_L^{LW}, γ_L^+, and γ_L^-). γ^{TOT} is total surface tension; γ^{AB} is AB components of surface tension. In this study, the UF membrane surface was treated as a solid, for the purpose of attaining surface energy parameters.

2.2. Feed water

The feed water in this study was obtained from the sand filter effluent of a waterworks in Nanjing, which receives raw water from the Yangtze River. The key characteristics of water quality are given in Table 1.

2.3. UF membrane

Hollow-fiber UF membrane, made of polyvinylidene fluoride (PVDF), was provided by Litree Purifying Technology Co., Ltd. (SuZhou, China), for use in this study. Detailed characteristics of the membrane are summarized in Table 2.

Table 2
Characteristics of UF membrane

Average molecular weight cutoff (Da)	50,000
Internal diameter (mm)	1.00
External diameter (mm)	1.66
Fiber length (m)	0.500
Effective surface area (m^2)	0.133
Filter type	Inside-out

2.4. Detection methods

2.4.1. Turbidity

Turbidity was measured using a Turbidimeter (2100 N, Hach, USA).

2.4.2. Ultraviolet absorbance (UV_{254})

Samples were pre-filtered through a 0.45-μm membrane (Millipore, USA) to remove particles prior to UV absorbance measurements and stored at 4℃ until further analysis. Ultraviolet (UV) absorbance at a wavelength of 254 nm (UV_{254}) was then measured using a UV/VIS spectrophotometer (EV300, Thermo Fisher, USA).

2.4.3. Dissolved organic carbon (DOC)

Dissolved organic carbon (DOC) was determined using a TOC analyzer (1030W, OI, USA). The samples were measured in five duplicates. The reported value was the average of the duplicate values, provided the relative percent difference between duplicate samples and calibration check standards was ≤ ± 5%. DOC was operationally defined as the organic carbon concentration of a sample filtered through a 0.45-μm membrane filter.

2.4.4. Colloid size

The average size of organic aggregates was determined using a dynamic light scattering measurement (Zeta sizer Nano ZS90, Malven Instruments Ltd, UK).

Table 1
Characteristics of feed water quality

Parameters	pH	Turbidity (NTU)	DOC (mg L^{-1})	UV_{254} (cm^{-1})	Colloid size (nm)	Zeta potential (mV)
	7.1	0.78	2.38	0.036	614.6	−11.8

2.4.5. Zeta potential

The zeta potential of the membrane surface was determined using a streaming potential analyzer (DelsaNano C/Solid Surface, Beckman, Germany). Zeta potential of the membrane surface was calculated from measured streaming potential, using the Helmholtz-Smoluchowski equation with the Fair-brother and Mastin substitution [19]. Zeta potential of the colloid particles was determined using a Nano particle size analyzer (Zetasizer Nano ZS90, Malven Instruments Ltd, UK).

2.4.6. Contact angle

The sessile drop method was used to measure the contact angle [27]. Contact angle measurement was performed using a standard contact angle goniometer (DSA100, KRUSS, Germany), an instrument that has image analysis attachments, including a video camera, monitor, and image analysis software. To determine the surface tension components of solid surfaces, two of the three probe liquids should be polar and the third should be nonpolar. In this experiment, we selected the following probe liquids: polar ultrapure water (Milli-Q system; Millipore Corp., USA), polar glycerol, and nonpolar diiodomethane. The glycerol and diiodomethane were of analytical grade (TCI, Shanghai, China).

2.4.7. Hydrophilic and hydrophobic components

The resins of Superlite DAX-8 (Supelco, USA), Amberlite XAD-4 (Rohm and Hass, Germany) and Amberlite IRA-958 (Rohm and Haas, Germany) were used to fractionate NOM into four groups [28]: hydrophobic fractions (HPO, DAX-8 adsorbable), transphilic fractions (TPI, XAD-4 adsorbable), negatively charged hydrophilic fractions (C-HPI, IRA-958 adsorbable), and neutral hydrophilic organic fractions (N-HPI, neither adsorbable). The resins were washed with methanol and deionized water prior to use in fractionation. The pH of water sample was adjusted to 2.0, prior to feeding into the DAX-8 absorption column (at a rate of 5 mL/min), the XAD-4 resin (at 15 mL/min), and Amberlite IRA-958 (at 10 mL/min). The absorbed organic fractions were then eluted from the resins of DAX-8, XAD-4, and IRA-958 using 0.1 mol/L NaOH, 1 mol/L NaOH, and 1 mol/L NaCl, respectively.

2.5. Pre-oxidation process

In this experiment, the UF system was used to investigate the effect of $KMnO_4$ pre-oxidation on membrane fouling. The bench-scale UF system is shown schematically in Fig. 1. Feed water was pumped using a peristaltic pump and mixed with $KMnO_4$, and then, the mixed water was filtered through a UF module. The transmembrane pressure (TMP) was recorded automatically using a pressure gauge.

In the pre-oxidation process, $KMnO_4$ may influence the characteristics of colloid both in feed water and membrane material, which may affect membrane fouling performance. To investigate the influence of $KMnO_4$ on membrane material and organic colloids, three parallel experiments therefore were performed as follows:

(1) Feed water without pre-oxidation was filtered by UF system using virgin membrane;
(2) Feed water without pre-oxidation was filtered by UF system using treated membrane. In this study, the treated membrane was attained by being soaked in potassium permanganate solution (0.4 mg L^{-1}) for 3 months;
(3) Feed water was firstly mixed with $KMnO_4$ at an optimized dose of 0.4 mg L^{-1}. The contact

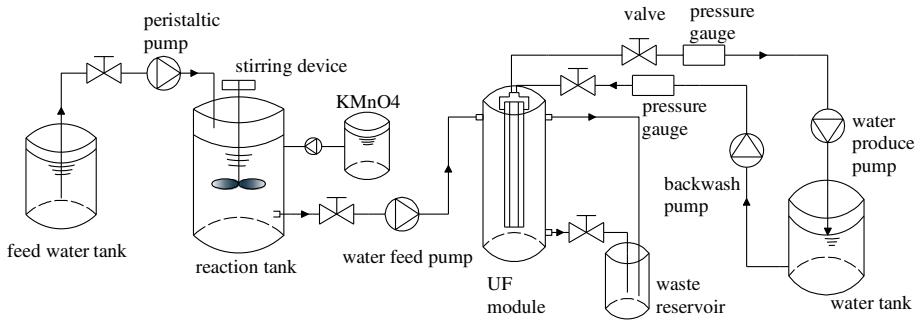

Fig. 1. Schematic diagram of $KMnO_4$/UF.

time of pre-oxidation was 10 min. And then, the mixed water was filtered by UF system using virgin membrane.

2.6. Membrane fouling experiment

Prior to the experiment, membranes were soaked in the pure water overnight and then were filtered using the pure water to achieve a stable permeate flux.

Pure water permeation flux: Ultrapure water (Milli-Q system, Millipore Corp., USA) was filtered through UF system under a fixed transmembrane pressure (TMP, −12 kP_a) at 24 ± 0.5℃, and the pure water permeation flux was recorded when the UF system was operated stably for 20 min.

TMP: Initial TMP (P_0) was measured by the filtration of pure water. After 2 h of pure water filtration, the feed water was pumped into the UF system, in which the permeate flux was fixed at 40 L m^2 h^{-1} using a peristaltic pump. The UF system was operated for 16 h. TMP of feed water sample (P_1) was compared with the initial TMP (P_0), which reflects the resistance of the UF system due to membrane fouling. The feed water, in the presence or the absence of $KMnO_4$ pretreatment, was introduced into the UF system, so as to investigate the TMP variations.

Membrane resistance: The resistance-in-series model was used to determine resistance according to the reported methods [27,28]:

$$J = \frac{\Delta P}{\mu R} \tag{10}$$

where J is the permeate flux (L m^2 h^{-1}), ΔP is the transmembrane pressure (Pa), μ is the viscosity of permeate (Pa s), and R is the total (overall) filtration resistance (m^{-1}).

In the case of filtration, the following equation was used [29]:

$$R = R_m + R_f = R_m + R_{rev} + R_{irr} \tag{11}$$

where R_m is the intrinsic membrane resistance (m^{-1}), determined by the experimental data relating to R in the filtration of pure water, and R_f is the total fouling resistance, which includes the physically reversible fouling resistance (R_{rev}, m^{-1}) and the physically irreversible fouling resistance (R_{irr}, m^{-1}) [27].

The value of experimental resistance, R_1, is determined from the experimental data at the end of filtration. The value of experimental resistance, R_2, is determined from the experimental data at the commencement of next filtration cycle after hydraulic cleaning. We obtain the formula for calculating resistance of R_{irr} and R_{rev}:

$$R_{irr} = R_2 - R_m \tag{12}$$

$$R_{rev} = R_1 - R_2 \tag{13}$$

From Eq. (10), we can obtain the formula for calculating resistance:

$$R = \frac{\Delta P}{J\mu} \tag{14}$$

where μ is 1.005×10^{-3} N S m^{-2} at the atmospheric temperature.

2.7. Analytical methods

To ensure the reliability of results, the experiment was performed in five parallels, so five replicate measurements of each sample were performed and the average value was determined ($p < 0.05$).

3. Results and discussion

3.1. Effect of $KMnO_4$ pre-oxidation on intrinsic membrane characteristics

3.1.1. Changes of contact angle and surface energy of membrane material

To understand how $KMnO_4$ pre-oxidation influences the intrinsic characteristics of membrane material so as to affect membrane fouling, the XDLVO approach was introduced to analyze the interaction energy profiles in the membrane material. Some parameters of virgin membrane and treated membrane, such as the contact angle and zeta potential, for calculating the interaction energy, are shown in Table 3. The calculated surface energy of membrane material is shown in Table 4.

As shown in Table 3, the contact angle between membrane surface and the probe liquid has been changed when membrane system was subjected to $KMnO_4$, which was attained by membrane being soaked in potassium permanganate solution (0.4 mg L^{-1}) for 3 months. The contact angle between ultrapure water and treated membrane was decreased compared with that of virgin membrane. Although the contact angle of treated membrane is still above 65°, reflecting the hydrophobic features of membrane

Table 3
Parameters of virgin membrane and treated membrane

	Contact angle (°)			
	Ultrapure water	Glycerol	Diiodomethane	Zeta potential (mV)
Virgin membrane	75.4 ± 4.2	59.3 ± 0.9	39.1 ± 1.1	−30.2
Treated membrane	66.8 ± 3.9	49.8 ± 0.7	48.9 ± 1.8	−43.4

Table 4
The surface energy of virgin and treated membrane material (mJ/m^2)

Surface energy	γ^{LW}	γ^{+}	γ^{-}	γ^{AB}	γ^{TOT}
Virgin membrane	40.045	0.855	5.073	4.164	44.209
Treated membrane	34.886	2.664	8.730	11.700	44.530

Table 5
Pure water permeation flux of membrane

Membrane	Pure water permeation flux (L m^2 h^{-1})
Virgin membrane	38.5
Treated membrane	45.8

material [30], the reduction of contact angle between polar ultrapure water or glycerol and membrane indicates the decrease of hydrophobicity of membrane material. The contact angle between nonpolar diiodomethane and membrane was increased, indicating the increasing polarity of membrane material. Such changes of contact angle are in favor of mitigating membrane fouling [31].

As shown in Table 4, the treated membrane exhibited a lower γ^{LW} value, indicating that the treated membrane presents more polar properties than virgin membrane [32]. The treated membrane also had a higher electron-acceptor component, corresponding to a high γ^{AB} value, when compared to virgin membrane. It has been proven that organic colloids with a weak electron-donor capability may interact unfavorably with surfaces that possess electron-acceptor functionality, thus reducing potentially attractive acid–base interaction [27]. Although the total surface energy had a smaller change, $KMnO_4$ pre-oxidation has changed the characteristics of membrane, i.e. the decrease of hydrophobicity, which alleviates membrane fouling as described in previous studies [33,34]. This is also in accordance with the result of contact angle.

3.1.2. Pure water permeation flux and resistance of membrane

The influence of $KMnO_4$ oxidation on the pure water permeation flux was further explored. Two membranes (virgin and treated) were investigated in parallel, and the results are shown in Table 5. As for the treated membrane, the pure water permeation flux increased, indicating that the increasing water permeability of UF due to the reduced hydrophobicity of membrane [35].

A comparison of membrane resistance (R_{irr} and R_{rev} noted as the percentage of the total membrane resistance on Y-axis), which was attained by filtering feed water without $KMnO_4$ pre-oxidation, is shown in Fig. 2. As can be seen, the membrane resistance was decreased in the UF system using the treated membrane. The reduction of irreversible fouling is more remarkable due to the changes of membrane characteristics. Previous research has shown that the pore size of membrane was diminished when it was soaked in potassium permanganate solution [10]. The influent of membrane system has residual $KMnO_4$ so as to affect the characteristics of membrane material, such as weakening the support of membrane pores [36]. This may cause less pore blockage of colloid, resulting in a remarkable reduction of irreversible fouling, while more colloids are intercepted on membrane surface to increase reversible fouling [37]. Some studies have indicated that functional groups on membrane surface have been changed when the membrane is subjected to oxidative solution, which includes the oxidation of unsaturated double bond to a single bond or higher level of hydroxyl group/C–H bond, indicating an increase in polarity or hydrophilicity of membrane material [10,27]. This may result in a higher interaction energy and a slighter membrane fouling [32].

3.2. Effect of $KMnO_4$ pre-oxidation on colloids

3.2.1. Changes of characteristics and surface energy of colloids in feed water

The characteristics of organic colloids in feed water with and without pre-oxidation are shown in Table 6. The contact angle between ultrapure water or glycerol and colloids was decreased, while that of

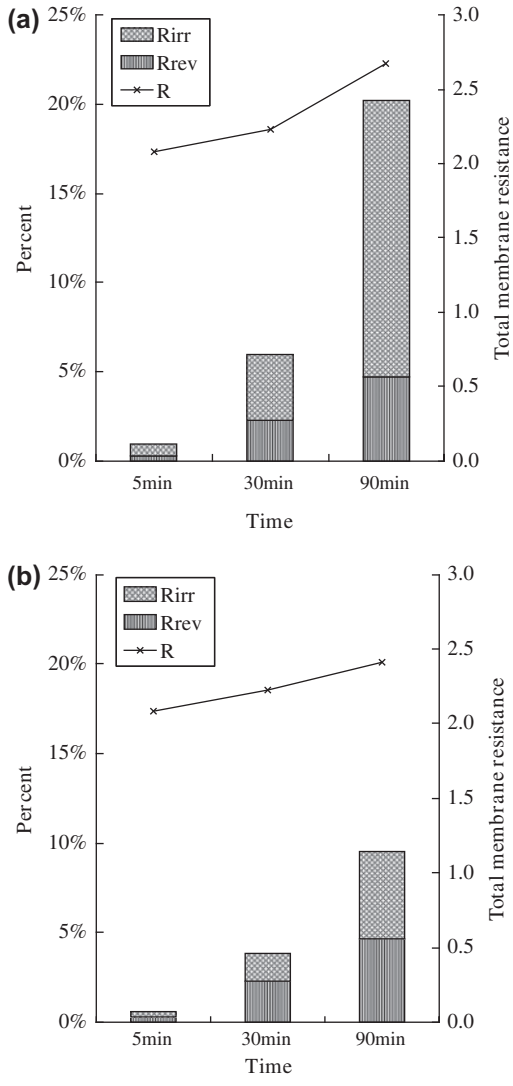

Fig. 2. The proportion of membrane resistance: (a) virgin membrane; (b) treated membrane (resistance unit: $\times 10^{12}$ m^{-1}).

diiodomethane was increased via $KMnO_4$ pre-oxidation. It indicates the increasing hydrophilicity and polarity of the colloids due to pre-oxidation, which may alleviate membrane fouling [27]. After $KMnO_4$ pre-oxidation, the value of colloid zeta potential was decreased due to the increased level of deprotonation [38], which may cause a higher repulsive force between colloids. Meanwhile, the negative charges on colloidal particles are increased by $KMnO_4$ pre-oxidation, and the organic coat that covers the colloid is also destroyed, causing a decrease in particle zeta potential [38]. The zeta potential of particles can influence membrane fouling [39], which is dependent on the total interaction energy. According to XDLVO theory, particle zeta potential only affects EL interaction energy. Previous studies have indicated that EL interaction is not a key factor in influencing the total interaction energy [34]. It is concluded that the influence of particle size on membrane fouling is greater than that of zeta potential [27]. The average colloidal size in the feed water was decreased after $KMnO_4$ pre-oxidation, fragmenting the macromolecules in the NOM into lower molecular weight organics [19]. The attachment of organic matter to membrane surface is the main cause of fouling. The macromolecular compounds as well as their colloidal aggregates usually have larger particle size, which contributes to significant organic fouling during low-pressure membrane filtration [27,40].

The calculated surface energy of colloids with and without $KMnO_4$ pre-oxidation is shown in Table 7. The value of γ^{LW} decreased and γ^{AB} increased after pre-oxidation, indicating that the oxidized colloid presents more hydrophilic than that without pre-oxidation [41]. Contributions of three interaction energies to total interaction energy are consistent with previous studies [42,43]. After pre-oxidation, values of LW, AB, and total interaction energy decreased 33.4,

Table 6
Water quality indexes and colloid parameters in raw feed water and pre-oxidated water

Indexes	pH	NTU	DOC (mg L^{-1})	UV_{254} (cm^{-1})	SUVA (L m^{-1} mg^{-1})
Raw feed water	7.1	0.88	2.78	0.036	1.295
Pre-oxidated water	7.3	0.48	2.49	0.032	1.285
Colloid parameters	Contact angle (°)			Zeta potential (mV)	Colloid size (nm)
	Ultrapure water	Glycerol	Diiodomethane		
Raw feed water	36.5 ± 2.4	53.9 ± 1.1	26.9 ± 0.7	−11.8	614.6
Pre-oxidated water	27.4 ± 2.3	40.3 ± 0.5	45.8 ± 0.5	−13.3	487.8

Table 7
The colloid surface energy and interaction energy between membrane and colloids in feed water with and without pre-oxidation (mJ/m^2)

Surface energy	γ^{LW}	γ^+	γ^-	γ^{AB}	γ^{TOT}
Raw feed water	45.452	0.110	50.428	4.717	50.169
Pre-oxidated water	36.581	0.886	50.044	13.320	49.901
Interaction energy	ΔG^{LW}	ΔG^{AB}	ΔG^{EL}	ΔG^{DLVO}	–
Raw feed water	−6.8778	−9.4687	0.0006	−16.3459	–
Pre-oxidated water	−4.5763	−6.2828	0.0003	−10.8588	–

33.6, and 33.6%, respectively. AB interaction energy denotes a significance of hydrogen bonding between two interfaces in aqueous. This result indicates that hydrogen bonding level is different in the feed water with and without $KMnO_4$ pre-oxidation. AB interaction energy is the major contributor to the total energy, indicating that hydrogen bonding plays a key role in holding the colloid aggregation together [44]. The reduction of AB interaction energy and total interaction energy can reduce colloids aggregation, leading to the mitigation of membrane fouling.

3.2.2. Effect on hydrophilic and hydrophobic fractions of NOM

NOM are fractionated into four fractions by water sample passing through a series of resins. The distribution of organic fraction in different water samples are shown in Fig. 3. As illustrated in Fig. 3, $KMnO_4$ pre-oxidation played an important role in the removal of DOC, mainly removing strongly hydrophobic organic compounds (HPO). The removal rate of hydrophobic fraction was therefore greater than that of hydrophilic fraction in UF system. The HPI/HPO ratio was increased after $KMnO_4$ pre-oxidation, indicating the increasing hydrophilicity of colloid in water. According to previous research, the absolute value of interaction energy of four fractions follows the following order: HPO > N-HPI > TPI > C-HPI. The removal of HPO can effectively reduce the interaction energy between colloid and membrane to mitigate membrane fouling [45].

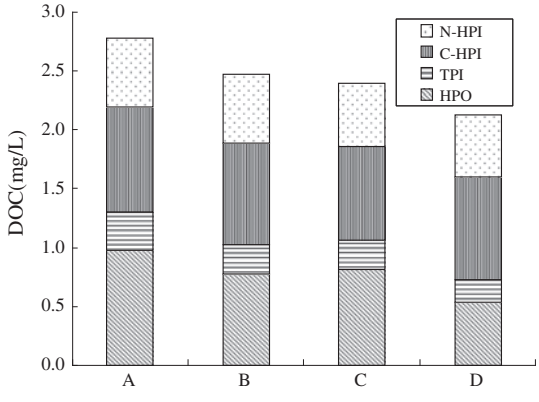

Fig. 3. Variations of the organic matter fraction in UF system with and without $KMnO_4$ pre-oxidation (A: feed water without $KMnO_4$ pre-oxidation; B: feed water with $KMnO_4$ pre-oxidation; C: effluent of UF system filtering feed water without $KMnO_4$ pre-oxidation; D: effluent of UF system filtering feed water with $KMnO_4$ pre-oxidation).

3.2.3. Membrane resistance variation

To investigate the influence of $KMnO_4$ pre-oxidation on TMP, the raw feed water and pre-oxidized feed water were filtered by UF system using virgin membrane. The result (shown in Fig. 4) indicates that the pre-oxidation of feed water using $KMnO_4$ mitigates membrane fouling. It was also observed several significant variations of the TMP during filtration of the pre-oxidated water. TMP increased in the initial period and subsequently had a slower rate of increase

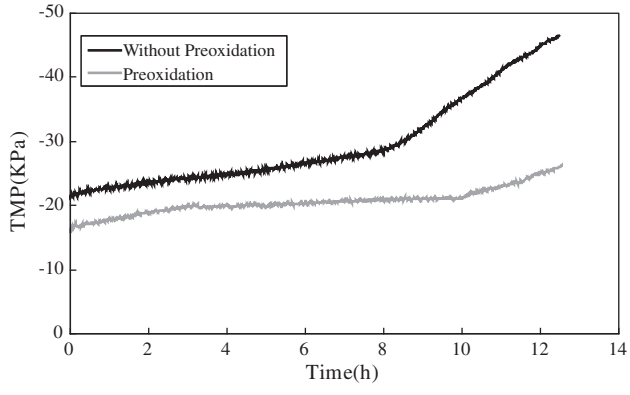

Fig. 4. TMP variation of two UF systems.

during the filtration. The increase of TMP at the initial stage is probably due to the adsorption of pollutants into the membrane pores [46], while its slower increase during the subsequent period demonstrates the formation of a loose filter cake during the course of filtration [47].

The proportion of membrane resistance is shown in Fig. 5. The total resistance increased more slowly, and a significant reduction of reversible resistance was found in the $KMnO_4$/UF system. The influence of $KMnO_4$ pre-oxidation on membrane fouling is considered as follows: one is the removal of organic foulants to mitigate membrane fouling; the other is the *in situ* formation of particulate manganese dioxide (MnO_2) [48]. MnO_2, as an intermediate, is incorporated into cake layer, bridging the colloids on the surface of membrane, which leads to the reduction of reversible fouling [16,19]. A portion of NOM is dislodged due to pre-oxidation, resulting in less foulants into membrane pore so as to reduce irreversible fouling. However, the macromolecular organic matter being oxidized to micromolecular fraction increases the probability of organic substance into membrane pore so as to cause irreversible fouling. It results in the unapparent reduction of irreversible fouling.

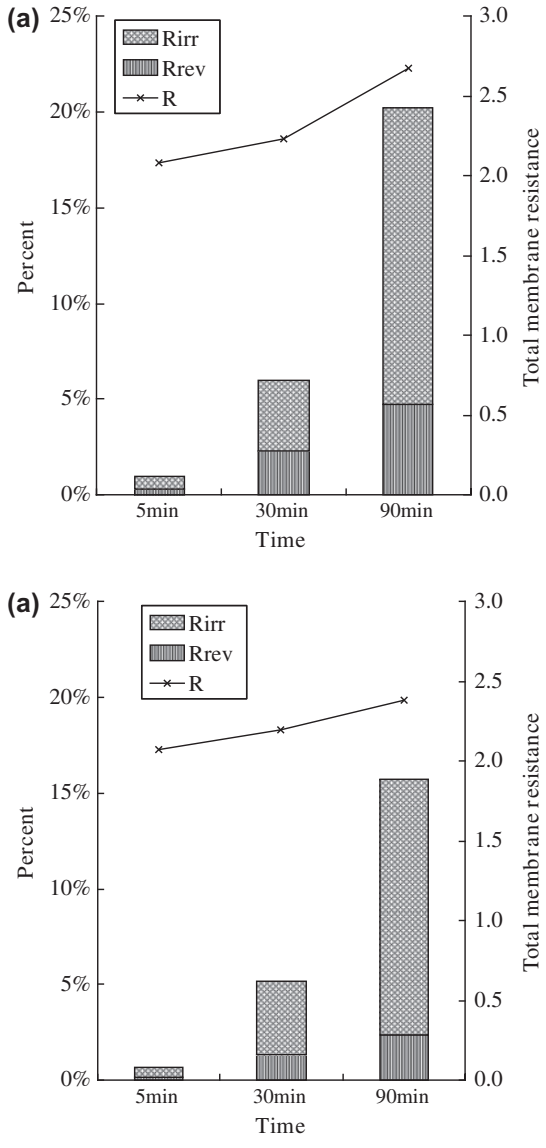

Fig. 5. The proportion of membrane resistance: (a) only UF system; (b) $KMnO_4$/UF system (resistance: ×10–12 m^{-1}).

It has been found that the reversible membrane fouling is relevant to AB interaction energy [27]. The result (shown in Table 7) indicates that the Lewis-acid and Lewis-base of water samples are changed due to pre-oxidation, which affects the value of the AB interaction. The reduction of AB interaction accounts for the lower TMP as well as the slower increasing rate of membrane fouling.

4. Conclusion

The result of this investigation demonstrated that $KMnO_4$ pre-oxidation of UF feed water was effective in migrating membrane fouling. $KMnO_4$ pre-oxidation effectively removed the hydrophobic fraction of NOM in water to mitigate membrane fouling. The result also showed that the TMP increased more slowly after $KMnO_4$ pre-oxidation, mainly due to the reduction of R_{rev}. The contact angle of membrane material was decreased when it was subjected to $KMnO_4$, resulting in a decrease in the interaction energy so as to mitigate membrane fouling. The pure water permeation flux of membrane was increased after $KMnO_4$ pre-oxidation.

Acknowledgements

Financial support was received from the National Natural Science Foundation of China (Project 51438006), Fundamental Research Funds for the Central Universities (Project 2014B07714) and a Project Funded by the Priority Academic Program Development of Jiangsu Higher Education Institutions.

References

[1] M. Elimelech, W.A. Phillip, The future of seawater desalination: Energy, technology, and the environment, Science 333 (2011) 712–717.
[2] M.M. Pendergast, E.M.V. Hoek, A review of water treatment membrane nanotechnologies, Energy Environ. Sci. 4 (2011) 1946–1971.

[3] F. Zaviska, P. Drogui, A. Grasmick, A. Azais, M. Héran, Nanofiltration membrane bioreactor for removing pharmaceutical compounds, J. Membr. Sci. 429 (2013) 121–129.
[4] R.D. Ambashta, M.E.T. Sillanpää, Membrane purification in radioactive waste management: A short review, J. Environ. Radioact. 105 (2012) 76–84.
[5] K. Kimura, Y. Hane, Y. Watanabe, G. Amy, N. Ohkuma, Irreversible membrane fouling during ultrafiltration of surface water, Water Res. 38 (2004) 3431–3441.
[6] R.B. Klijn, W.G.J. van der Meer, H. Vriezen, F.H.J. van Ekkendonk, Surface water treatment with Zenon microfiltration membranes: Minimisation of energy and chemical use, Desalination 131 (2000) 337–343.
[7] S.R. Chae, H. Yamamura, K. Ikeda, Y. Watanabe, Comparison of fouling characteristics of two different poly-vinylidene fluoride microfiltration membranes in a pilot-scale drinking water treatment system using pre-coagulation/sedimentation, sand filtration, and chlorination, Water Res. 42 (2008) 2029–2042.
[8] J.M. Laîné, D. Vial, P. Moulart, Status after 10 years of operation-overview of UF technology today, Desalination 131 (2000) 17–25.
[9] H. Yamamura, S. Chae, K. Kimura, Y. Watanabe, Transition in fouling mechanism in microfiltration of a surface water, Water Res. 41 (2007) 3812–3822.
[10] T. Lin, S.L. Pan, W. Chen, S. Bin, Role of preoxidation, using potassium permanganate, for mitigating membrane fouling by natural organic matter in an ultrafiltration system, Chem. Eng. J. 223 (2013) 487–496.
[11] I. Sutzkover-Gutman, D. Hasson, R. Semiat, Humic substances fouling in ultrafiltration processes, Desalination 261 (2010) 218–231.
[12] S.L. Shao, H. Liang, F.S. Qu, H.R. Yu, K. Li, G.B. Li, Fluorescent natural organic matter fractions responsible for ultrafiltration membrane fouling: Identification by adsorption pretreatment coupled with parallel factor analysis of excitation-emission matrices, J. Membr. Sci. 464 (2014) 33–42.
[13] A.R. Costa, M.N. Depinho, M. Elimelech, Mechanisms of colloidal natural organic matter fouling in ultrafiltration, J. Membr. Sci. 281 (2006) 716–725.
[14] S. Lee, K. Lee, W.M. Wan, Y. Choi, Comparison of membrane permeability and a fouling mechanism by pre-ozonation followed by membrane filtration and residual ozone in membrane cells, Desalination 178 (2005) 287–294.
[15] W. Gao, H. Liang, J. Ma, M. Han, Z.L. Chen, Z.S. Han, G.B. Li, Membrane fouling control in ultrafiltration technology for drinking water production: A review, Desalination 272 (2011) 1–8.
[16] J.J. Chen, H.H. Yeh, The mechanisms of potassium permanganate on algae removal, Water Res. 39 (2005) 4420–4428.
[17] J.D. Plummer, J.K. Edzwald, Effect of ozone on algae as precursors for trihalomethane and haloacetic acid production, Environ. Sci. Technol. 35 (2001) 3661–3668.
[18] J.D. Plummer, J.K. Edzwald, Effects of chlorine and ozone on algal cell properties and removal of algae by coagulation, J. Water SRT-Aqua 21 (2002) 307–318.
[19] H. Liang, Y.L. Yang, W.J. Gong, X. Li, G.B. Li, Effect of pretreatment by permanganate/chlorine on algae fouling control for ultrafiltration (UF) membrane system, Desalination 222 (2008) 74–80.
[20] T. Lin, L. Li, W. Chen, S.L. Pan, Effect and mechanism of preoxidation using potassium permanganate in an ultrafiltration membrane system, Desalination 286 (2012) 379–388.
[21] W. Song, V. Ravindran, B.E. Koel, M. Pirbazari, Nanofiltration of natural organic matter with H_2O_2/UV pretreatment: Fouling mitigation and membrane surface characterization, J. Membr. Sci. 241 (2004) 143–160.
[22] J.A. Brant, A.E. Childress, Assessing short-range membrane-colloid interactions using surface energetics, J. Membr. Sci. 203 (2002) 257–273.
[23] M.J.D. Bower, T.L. Bank, R.F. Giese, C.G. van Oss, Nanoscale forces of interaction between glass in aqueous and non-aqueous media: A theoretical and empirical study, Colloids Surf., A 362 (2010) 90–96.
[24] L. Feng, X.F. Li, G.C. Du, J. Chen, Adsorption and fouling characterization of *Klebsiella oxytoca* to microfiltration membranes, Process Biochem. 44 (2009) 1289–1292.
[25] C.Y. Tang, T.H. Chong, A.G. Fane, Colloidal interactions and fouling of NF and RO membranes: A review, Adv. Colloid Interface Sci. 164 (2011) 126–143.
[26] S. Kim, M. Marion, B.H. Jeong, E.M.V. Hoek, Crossflow membrane filtration of interacting nanoparticle suspensions, J. Membr. Sci. 284 (2006) 361–372.
[27] T. Lin, Z.J. Lu, W. Chen, Interaction mechanisms and predictions on membrane fouling in an ultrafiltration system, using the XDLVO approach, J. Membr. Sci. 461 (2014) 39–48.
[28] T. Lin, B. Shen, W. Chen, X.B. Zhang, Interaction mechanisms associated with organic colloid fouling of ultrafiltration membrane in a drinking water treatment system, Desalination 332 (2014) 100–108.
[29] A.R. Rajabzadeh, C. Moresoli, B. Marcos, Fouling behavior of electroacidified soy protein extracts during cross-flow ultrafiltration using dynamic reversible–irreversible fouling resistances and CFD modeling, J. Membr. Sci. 361 (2010) 191–205.
[30] S. Rüttermann, T. Beikler, R. Janda, Contact angle and surface free energy of experimental resin-based dental restorative materials after chewing simulation, Dent. Mater. 30 (2014) 702–707.
[31] H.C. Kim, B.A. Dempsey, Removal of organic acids from EfOM using anion exchange resins and consequent reduction of fouling in UF and MF, J. Membr. Sci. 364 (2010) 325–330.
[32] X. Kang, W.X. Mao, H. Xia, T.D. Waite, W.X. Hua, Combined effect of membrane and foulant hydrophobicity and surface charge on adsorptive fouling during microfiltration, J. Membr. Sci. 373 (2011) 140–151.
[33] X.Y. Su, Y. Tian, H. Li, C.N. Wang, New insights into membrane fouling based on characterization of cake sludge and bulk sludge: An especial attention to sludge aggregation, Bioresour. Technol. 128 (2013) 586–592.
[34] M. Farahat, T. Hirajima, K. Sasaki, Adhesion of *Ferroplasma acidiphilum* onto pyrite calculated from the extended DLVO theory using the van

Oss-Good-Chaudhury approach, J. Colloid Interface Sci. 349 (2010) 594–601.
[35] G. Hurwitz, G.R. Guillen, E.M.V. Hoek, Probing polyamide membrane surface charge, zeta potential, wettability, and hydrophilicity with contact angle measurements, J. Membr. Sci. 349 (2010) 349–357.
[36] H. Xu, W. Chen, H.Y. Xiao, X.H. Hu, Stability of an ultrafiltration system for drinking water treatment, using chlorine for fouling control, Desalination 336 (2014) 187–195.
[37] H. Huang, N. Lee, T. Young, A. Gary, J.C. Lozier, J.G. Jacangelo, Natural organic matter fouling of low-pressure, hollow-fiber membranes: Effects of NOM source and hydrodynamic conditions, Water Res. 41 (17) (2007) 3823–3832.
[38] A.E. Childress, M. Elimelech, Effect of solution chemistry on the surface charge of polymeric reverse osmosis and nanofiltration membranes, J. Membr. Sci. 119 (1996) 253–268.
[39] A.M. Kusuma, Q.X. Liu, H.B. Zeng, Understanding interaction mechanisms between pentlandite and gangue minerals by zeta potential and surface force measurements, Miner. Eng. 69 (2014) 15–23.
[40] Y.W. Liu, X. Li, Y.L. Yang, W.L. Ye, S.Y. Ji, J.W. Ren, Z.W. Zhou, Analysis of the major particle-size based foulants responsible for ultrafiltration membrane fouling in polluted raw water, Desalination 347 (2014) 191–198.
[41] A. Subramani, X.F. Huang, E.M.V. Hoek, Direct observation of bacterial deposition onto clean and organic-fouled polyamide membranes, J. Colloid Interface Sci. 336 (2009) 13–20.
[42] V.I. Syngouna, C.V. Chrysikopoulos, Cotransport of clay colloids and viruses in water saturated porous media, Colloids Surf., A 416 (2013) 56–65.
[43] S.C. Zhen, Y.Q. Yan, G.B. Yu, M.R. Min, L. Jing, Z.Y. Xia, Y.Z. Lian, X.W. Ying, Effect of pH and shear force on flocs characteristics for humic acid removal using poly ferric aluminum chloride-organic polymer dual-coagulants, Desalination 281 (2011) 243–247.
[44] H.Y. Yu, H.J. Lin, M.J. Zhang, H.C. Hong, Y.M. He, F.Y. Wang, L.H. Zhao, Membrane fouling in a submerged membrane bioreactor with focus on surface properties and interactions of cake sludge and bulk sludge, Bioresour. Technol. 169 (2014) 213–219.
[45] W.W. Huang, H.Q. Chu, B.Z. Dong, Understanding the fouling of algogenic organic matter inmicrofiltration using membrane-foulant interaction energy analysis: Effects of organic hydrophobicity, Colloids Surf., B 122 (2014) 447–456.
[46] K. Katsoufidou, S.G. Yiantsios, A.J. Karabelas, A study of ultrafiltration membrane fouling by humic acids and flux recovery by backwashing: Experiments and modeling, J. Membr. Sci. 266 (2005) 40–50.
[47] G.V. Korshin, C.W. Li, M.M. Benjamin, Monitoring the properties of natural organic matter through UV spectroscopy: A consistent theory, Water Res. 31(7) (1997) 1787–1795.
[48] J.Y. Tian, M. Ernst, F.Y. Cui, M. Jekel, $KMnO_4$ pre-oxidation combined with $FeCl_3$ coagulation for UF membrane fouling control, Desalination 320 (2013) 40–48.